

towards high ϵ . In spite of this deficiency, the \bar{T}_ϵ trajectories do resemble hyperbolas so that the simple model may serve for a qualitative discussion of the phase behavior of such quinary mixtures. One could easily improve the model by adding quadratic terms to eq 1 and 2. This, however, would introduce an additional parameter depending on δ that would have to be determined for each mixture.

VII. Further Discussion

In the above mixture one finds $\bar{T}_N > \bar{T}_I$, thus $\epsilon^* > 0$, and, accordingly, both types of hyperbolas. Since, furthermore, both \bar{T}_N and \bar{T}_I lie between the melting and boiling points of the mixture, one finds both the nonionic and the ionic branches. If \bar{T}_N or \bar{T}_I lie either below the melting point or above the boiling point, the corresponding branches will enter the "experimental window" only at intermediate values of δ , if at all. An example is the combination of a $C_{12}E_7$ with a standard single-tailed anionic amphiphile, for which \bar{T}_I lies well below the melting point. For this case the model predicts that one finds nonionic branches only, ascending at low ϵ and descending at high ϵ .

If, like in Schulman type of mixtures, that is, with a short chain alcohol as nonionic amphiphile and a standard single-tailed ionic amphiphile, both \bar{T}_N and \bar{T}_I lie below the melting point, the model predicts in agreement with experience that one should find three-phase bodies only at intermediate values of δ (and $\epsilon > 0$), but neither at $\delta = 0$ nor at $\delta = 100$.

If one applies cationic instead of anionic amphiphiles, one expects no qualitative but only quantitative differences due to the different polarity of the ionic head groups.

VIII. Conclusion

It is suggested to study the phase behavior of quinary mixtures of water, oil, a nonionic amphiphile, an ionic amphiphile, and salt by tracing that point \bar{X} at which the three-phase body of the

mixture touches the homogeneous solution. At constant fraction α of the oil in the mixture of oil and brine, \bar{X} is unambiguously defined by its temperature \bar{T} and the fraction $\bar{\gamma}$ of the two amphiphiles in the mixture. Both \bar{T} and $\bar{\gamma}$ depend sensitively but systematically on the nature of the components, as well as on the fraction δ of the ionic in the mixture of the two amphiphiles and the brine concentration ϵ .

It is suggested to present \bar{T} in $T-\delta-\epsilon$ space and $\bar{\gamma}$ in $\gamma-\delta-\epsilon$ space. The first representation gives the temperature at which to search for a three-phase body and the latter which efficiency of the amphiphiles to expect. It is shown that \bar{T} lies on a surface in $T-\delta-\epsilon$ space, the shape of which is determined by the interplay between the \bar{T} trajectory of the A-B-C-E and that of the A-B-D-E mixture. The \bar{T}_ϵ trajectories along this surface resemble hyperbolas that diverge at a pole $0 < \delta^* < 100$ wt %. Accordingly, the trajectories for $\delta < \delta^*$ can be considered as nonionic, those for $\delta > \delta^*$ as ionic branches.

On the basis of such studies, an empirical description of the phase behavior is presented that permits qualitative predictions with respect to the dependence of the phase behavior on the nature of the components and the variables δ and ϵ . This will be demonstrated on a number of representative mixtures in a forthcoming paper.¹³

Acknowledgment. We are indebted to Mrs. H. Frahm, Mr. A. Ellrott, Mr. B. Faulhaber, Mr. T. Lieu, and Mr. R. Maliska for their assistance with the experiments, Mr. D. Luckmann for drawing the figures, and to the German Federal Ministry for Research and Technology (BMFT) for financial support (Grant No. 0326315 B).

Registry No. AOT, 577-11-7; $C_{12}E_4$, 5274-68-0; NaCl, 7647-14-5; decane, 124-18-5.

(13) Kahlweit, M.; Strey, R., in preparation.

Kinetics of CO Oxidation by O₂ or NO on Rh(111) and Rh(100) Single Crystals

C. H. F. Peden,* D. W. Goodman, D. S. Blair, P. J. Berlowitz,

Sandia National Laboratories, Albuquerque, New Mexico 87185

G. B. Fisher, and S. H. Oh

Physical Chemistry Department, General Motors Research Laboratories, Warren, Michigan 48090-9055
(Received: April 9, 1987)

The oxidation of CO by O₂ or NO over Rh(111) and Rh(100) single crystals has been studied in a high-pressure reaction-high-vacuum surface analysis apparatus. Steady-state catalytic activity as a function of temperature and partial pressures of CO, O₂, and NO has been measured. The CO-O₂ reaction was found to be insensitive to the structure of the surface as evidenced by the identical rates, activation energies, and partial pressure dependencies measured on the two single-crystal surfaces. Both surfaces deactivated at high O₂ partial pressures due to the formation of a near-surface oxide (probably Rh₂O₃) which is catalytically inactive for this reaction. The deactivation occurred at a slightly lower O₂ partial pressure on Rh(100), likely due to the relative ease of oxygen diffusion through this surface leading to more rapid bulk oxidation. Unlike the CO-O₂ reaction, CO oxidation by NO was very sensitive to the geometric structure of the surface. This behavior was evident in all kinetic parameters measured on the two surfaces. The kinetic data obtained on Rh(111) agree quantitatively with a surface chemistry model previously developed for this reaction. The model predicts that the rate is limited by the formation of N₂ from the recombination of adsorbed N atoms, and that the surface, under steady-state reaction conditions, is covered largely with adsorbed N atoms and smaller amounts of adsorbed NO. On Rh(100) the data are consistent with a reaction rate limited by the formation of N₂ from the surface reaction of adsorbed NO and N atoms.

1. Introduction

The catalyzed oxidation of CO by O₂, or by the simultaneous reduction of NO, is an important process in the pollution control of combustion products. Rhodium has shown good activity for reducing NO¹ and oxidizing CO by O₂.² As such, research to

better understand transition-metal catalysts and, in particular, the activity of Rh for these reactions is continuing.³⁻⁸ Oh et al.⁹

(1) Schlatter, J. C.; Taylor, K. C. *J. Catal.* 1977, 49, 42.

(2) Taylor, K. C. *Ind. Eng. Chem. Prod. Res. Dev.* 1976, 15, 264.

have interpreted the kinetics of the CO–O₂ and CO–NO reactions by using mathematical models which take into account the rates of each elementary step of the reactions. Such models, utilizing parameters obtained in ultra-high-vacuum (UHV) surface science experiments, can quantitatively account for the measured macroscopic kinetics obtained on single crystals at realistic high pressures. Measurements of the rate of CO oxidation at low pressure (<10⁻⁴ Torr) over Pd single crystals¹⁰ and more recently at elevated pressures (10–100 Torr) on Ir(111) and Ir(110)¹¹ suggest that this reaction is insensitive to changes in the surface structure of the catalyst. In support of this, specific rates of CO oxidation obtained on Rh(111) were identical with those measured on a supported Rh/Al₂O₃ catalyst.⁹ Modelling CO oxidation with a Langmuir–Hinshelwood type reaction between adsorbed atomic oxygen and molecular CO, in which the surface is predominantly covered with adsorbed CO, successfully predicted the absolute rates of reaction as well as the pressure dependence on the single-crystal and supported catalysts.⁹ It was determined in this study that the rate-determining step of the reaction is the dissociative adsorption of O₂ which is effectively blocked by the high surface coverages of CO. As expected from the structure insensitivity, similar results were obtained by Daniel and White¹² who performed low-pressure steady-state measurements of CO oxidation over Rh(100). These authors concluded that, for CO partial pressures approximately equal to or greater than O₂ partial pressures at temperatures around 450 K, an accumulation of CO on the surface blocks the adsorption of O₂, thereby making oxygen adsorption rate-limiting. At significantly lower CO partial pressures, the surface coverage of CO was reduced and the kinetics entered a regime in which the rate is limited by the adsorption of CO. We report here a parallel study of the CO–O₂ reaction on single-crystal Rh(111) and Rh(100) in which structure insensitivity for steady-state reaction is again confirmed. There are, however, interesting differences in the O₂/CO ratio needed to deactivate the two single-crystal catalysts which may be related to the ease with which the two surfaces oxidize.

In contrast to the structure insensitivity of the CO–O₂ reaction, recent experimental and modelling studies by Oh et al.⁹ have shown that the CO–NO reaction exhibits substantially different kinetic behavior between supported Rh/Al₂O₃ and Rh(111). These authors postulate that the structure sensitivity of the CO–NO reaction is due to drastically different rates of NO dissociation on the two types of Rh catalysts. On Rh(111) the rate is limited by Langmuir–Hinshelwood reactions to form N₂, whereas on the supported catalyst the rate-limiting step was judged to be the dissociation of NO. The model calculations utilized two competing

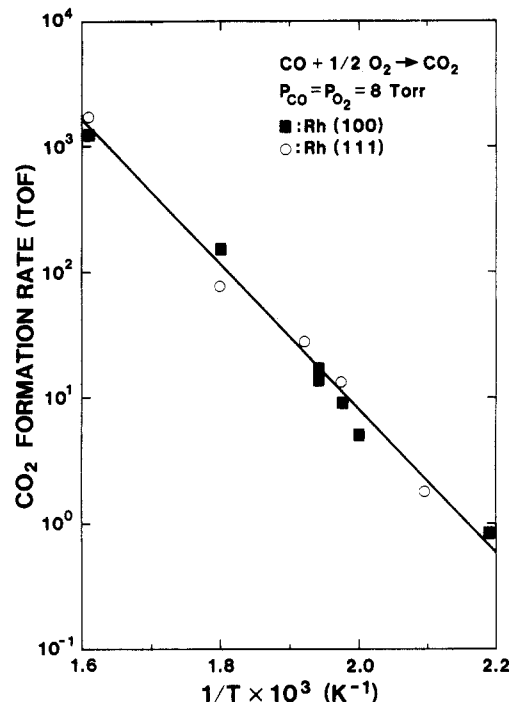


Figure 1. Arrhenius plot of the CO–O₂ reaction rates on Rh(111) and Rh(100) surfaces. $P(\text{CO}) = P(\text{O}_2) = 8$ Torr.

routes to the formation of N₂ on the surface defined as $\delta\text{-N}_2$ ($\text{NO}_a + \text{N}_a \rightarrow \text{N}_2 + \text{O}_a$) dominant at low temperatures (<550 K), and as $\beta\text{-N}_2$ ($\text{N}_a + \text{N}_a \rightarrow \text{N}_2$) dominant at high temperatures. The surface chemistry reaction model showed good agreement between predicted and measured rates of reaction on Rh(111) as well as the reaction rate dependence with NO and CO pressure. We report here measurements of the CO–NO reaction kinetics on Rh(100) and comparisons with those on Rh(111) which confirm the structure sensitive nature of this reaction.

2. Experimental Section

The apparatus used for these experiments has been described in detail previously.¹³ Briefly, the system consists of an UHV surface analysis chamber connected to a high-pressure reaction chamber. The single-crystal samples, mounted on the arm of a retractable bellows, can be transferred in vacuo from the reactor to the analysis chamber. The Rh(100) sample was a disk measuring 0.65 cm in diameter by 0.06 cm thick whereas the Rh(111) crystal was elliptically shaped measuring 0.91 by 0.58 cm and 0.09 cm thick. Both samples were heated resistively by two high-purity 0.020-in. tungsten leads spot-welded to the rear of the crystals. The temperature measurement was made by chromel–alumel thermocouples spot-welded to the edges of the crystals.

Auger electron spectroscopy (AES) was used to characterize the crystal surfaces before and after high-pressure reaction to ensure atomic cleanliness before reaction and to investigate the chemical nature of the surface as a function of variable reaction conditions. Clean Rh surfaces could be conveniently obtained by running a CO–O₂ reaction in the high-pressure reactor, with any residual oxygen removed by heating the crystal to 1200 K. Gas chromatography with flame ionization detection (FID) was used for the analysis of CO and CO₂ which were catalytically converted to methane before detection. Rates of reaction are expressed as turnover frequencies (TOF) defined as the number of CO₂ molecules formed per surface metal atom per second. Surface Rh atoms are determined from the measured area of the crystals and the known atomic densities of the Rh(100) (1.45×10^{15} atoms/cm²)¹⁴ and Rh(111) (1.60×10^{15} atoms/cm²)¹⁵ surfaces.

- (3) Bonzel, H. P.; Ku, R. *Surf. Sci.* **1972**, *33*, 91.
 (4) (a) Matsushima, T.; Almy, D. B.; Foyt, D. C.; Close, J. S.; White, J. M. *J. Catal.* **1975**, *39*, 277. (b) Matsushima, T.; Mussett, C. J.; White, J. M. *J. Catal.* **1976**, *41*, 397. (c) Matsushima, T.; Almy, D. B.; White, J. M. *Surf. Sci.* **1977**, *67*, 89. (d) Matsushima, T.; White, J. M. *Surf. Sci.* **1977**, *67*, 122. (e) White, J. M.; Golchat, A. *J. Chem. Phys.* **1977**, *66*, 5744. (f) Campbell, C. T.; White, J. M. *Appl. Surf. Sci.* **1978**, *1*, 347. (g) Campbell, C. T.; Shi, S.-K.; White, J. M. *Appl. Surf. Sci.* **1979**, *2*, 382.
 (5) (a) Hecker, W. C.; Bell, A. T. *J. Catal.* **1983**, *84*, 200. (b) Hecker, W. C. Ph.D. Thesis, University of California, Berkeley, 1982.
 (6) (a) Kiss, J. T.; Gonzalez, R. D. *J. Phys. Chem.* **1984**, *88*, 898. (b) McClory, M. M.; Gonzalez, R. D. *J. Phys. Chem.* **1986**, *90*, 628.
 (7) (a) Lintz, H.-G.; Weisker, T. *Appl. Surf. Sci.* **1985**, *24*, 251. (b) Lintz, H.-G.; Weisker, T. *Appl. Surf. Sci.* **1985**, *24*, 259. (c) Lintz, H.-G.; Weisker, T. *Appl. Surf. Sci.* **1985**, *24*, 268.
 (8) (a) Fisher, G. B.; Oh, S. H.; Carpenter, J. E.; DiMaggio, C. L.; Schmeig, S. J.; Goodman, D. W.; Root, T. W.; Schwartz, S. B.; Schmidt, L. D. In *Proceedings of the International Conference on Catalysis and Automotive Emission Control*; Frennet, H., Cruca, A., Eds.; Elsevier: Amsterdam, 1987; p 215. (b) Goodman, D. W.; Peden, C. H. F. *J. Phys. Chem.* **1986**, *90*, 4839. (c) Schwartz, S. B.; Schmidt, L. D.; Fisher, G. B. *J. Phys. Chem.* **1986**, *90*, 6194. (d) Schwartz, S. B.; Fisher, G. B.; Schmidt, L. D., to be submitted for publication. (e) Fisher, G. B.; Oh, S. H.; DiMaggio, C. L.; Schmeig, S. J.; Goodman, D. W.; Peden, C. H. F. In *Proceedings of the Ninth International Congress on Catalysis*; Ternan, M., Ed., in press.
 (9) Oh, S. H.; Fisher, G. B.; Carpenter, J. E.; Goodman, D. W. *J. Catal.* **1986**, *100*, 360.
 (10) Engel, T.; Ertl, G. *Adv. Catal.* **1979**, *28*, 1.
 (11) Berlowitz, P. J.; Peden, C. H. F.; Goodman, D. W. *J. Phys. Chem.*, submitted for publication.
 (12) Daniel, W. M.; White, J. M. *Int. J. Chem. Kinet.* **1985**, *17*, 413.

(13) Goodman, D. W.; Kelley, R. D.; Madey, T. E.; Yates, J. T., Jr. *J. Catal.* **1980**, *63*, 226.

(14) Fisher, G. B.; Schmeig, S. J. *J. Vac. Sci. Technol. A* **1983**, *1*, 1064.

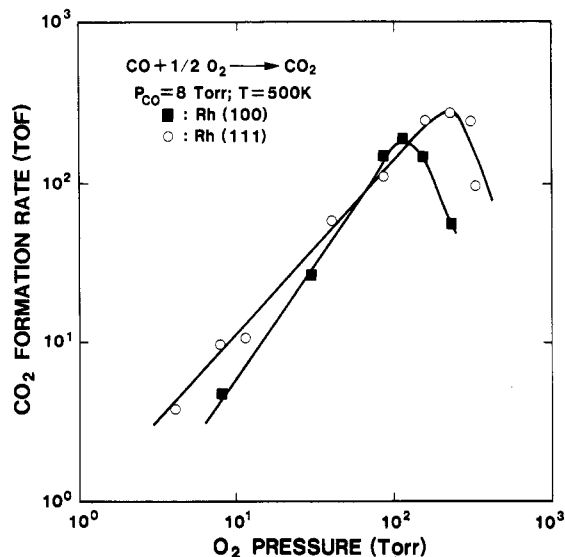


Figure 2. Rates of CO_2 formation from the $\text{CO}-\text{O}_2$ reaction on Rh(111) and Rh(100) as a function of O_2 partial pressure. $P(\text{CO}) = 8$ Torr; $T = 500$ K.

A typical experiment proceeded in the following manner: (1) the Rh surface was cleaned and checked by AES; (2) the sample was retracted and isolated from the UHV analysis chamber; (3) the reaction gases were introduced into the reaction chamber to the desired levels; (4) the sample was resistively heated to the reaction temperature for a specified time with reaction terminated by quenching the crystal, i.e., the reactions were done in batch mode; (5) the reactant and product gases were allowed to equilibrate for approximately 15 min before small aliquots were injected into the gas chromatograph; (6) the reactor was evacuated and the sample reintroduced into the analysis chamber; (7) the sample was heated to at least 500 K to remove residual CO (which will decompose in the electron beam of the Auger analyzer) before AES spectra were again obtained.

O_2 (99.99%), NO (99.0%), and CO (99.99%) gases were obtained from Matheson Gas Products. CO was further purified by passing the gas through a glass-wool trap held at liquid nitrogen temperature to remove volatile metal carbonyls. Postreaction surface analysis as described above indicated the presence of only adsorbed oxygen and nitrogen.

3. Results

3.1. $\text{CO}-\text{O}_2$ Reaction. Arrhenius plots of the specific rates, or turnover frequencies, of the CO oxidation reaction over Rh(100) and Rh(111) are shown in Figure 1. At equal partial pressures of CO and O_2 (8.0 Torr), the reaction rates are virtually identical on the two surfaces, yielding an apparent activation energy of approximately 25.4 kcal/mol. There is good agreement (within a factor of about 1.5) between these data and the rates obtained on supported 0.01% Rh/ Al_2O_3 catalysts as shown in ref 9.

The dependence of the rate of the $\text{CO}-\text{O}_2$ reaction, at 500 K and a CO partial pressure of 8.0 Torr, on the partial pressure of oxygen is shown in Figure 2 for both the (100) and (111) surfaces. The reaction rate for both surfaces increases linearly at low oxygen partial pressures. This first-order dependence is altered at high oxygen pressures where the rates rollover and become negative order with respect to oxygen pressure. Note that this rollover occurs at different oxygen partial pressures on the two single-crystal surfaces.

The level of residual surface oxygen remaining on the surface after reaction was measured by the ratio of the $\text{O}(\text{KLL})$ to $\text{Rh}(\text{MNN})$ Auger transitions at 510 and 302 eV, respectively. Figure 3 shows this ratio for reactions at 500 K and CO partial pressures of 8.0 Torr as a function of oxygen partial pressure for both single-crystal surfaces. The (100) surface shows gradually in-

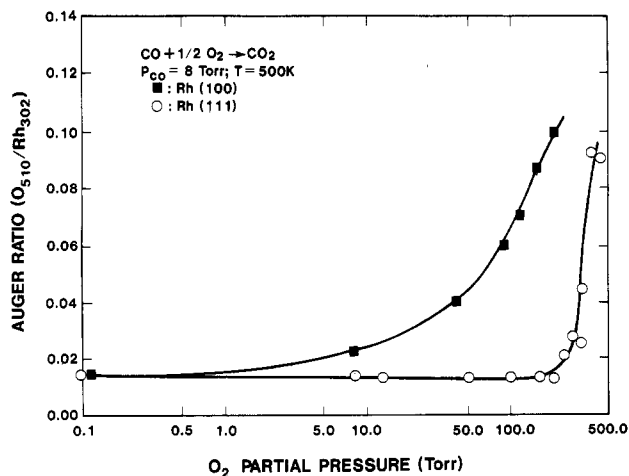


Figure 3. Amount of adsorbed oxygen remaining on the surface of Rh(111) and Rh(100) after reaction as a function of O_2 partial pressure. $P(\text{CO}) = 8$ Torr; $T = 500$ K.

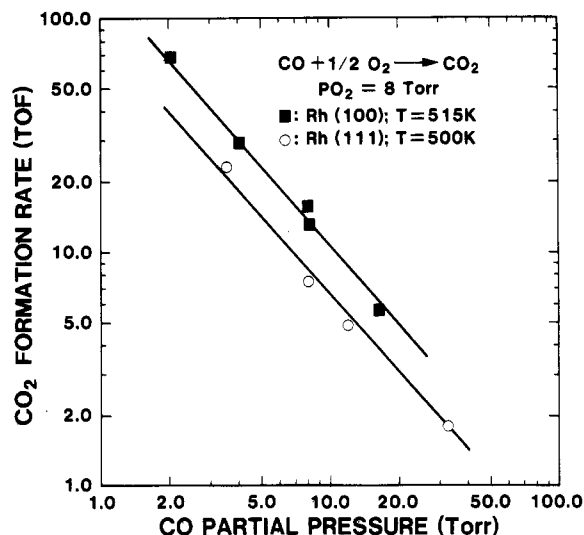


Figure 4. CO_2 formation rates from the $\text{CO}-\text{O}_2$ reaction on Rh(111) and Rh(100) as a function of CO partial pressure. $P(\text{O}_2) = 8$ Torr; $T[\text{Rh}(111)] = 500$ K; $T[\text{Rh}(100)] = 515$ K.

creasing amounts of residual oxygen with increasing oxygen partial pressures. At pressures greater than 75 Torr (O_2/CO ratio $\approx 10:1$), coinciding with the oxygen pressure at which the rate rolls over from positive to negative order (Figure 2), the surface oxygen level increases dramatically. On the (111) surface, no increase over a base oxygen level is observed until the oxygen partial pressure is greater than 230 Torr, or an O_2/CO ratio greater than 30:1. Again, this increase in the residual oxygen signal occurs at pressures above which the CO oxidation rate drops in Figure 2 on the Rh(111) surface. (In an earlier publication from this laboratory,^{8b} it was suggested that residual oxygen was not detectable on a deactivated Rh(111) catalyst surface. In fact, postreaction AES studies at oxygen pressures sufficient to deactivate the surface (compare Figures 3a and 5a in ref 8b) were not performed in the earlier work.)

The kinetic order of the CO oxidation reaction with respect to CO partial pressure for both single-crystal surfaces is shown in Figure 4. Note that the temperature at which these measurements were made was different for Rh(111) (500 K) and Rh(100) (515 K). As can be seen in the figure, negative first-order dependence on CO partial pressure is observed for both surfaces. The pressure dependencies of both reactants measured on the single-crystal catalysts are in good qualitative agreement with previous measurements on supported Rh/ SiO_2 ,¹⁶ and in quantitative agreement with studies on supported Rh/ Al_2O_3 ⁹ catalysts.

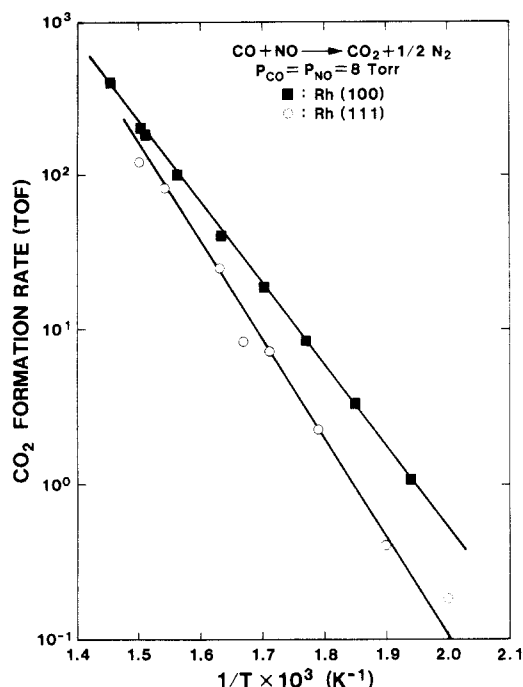


Figure 5. Arrhenius plot of the CO_2 formation rate from the CO-NO reaction on $\text{Rh}(111)$ and $\text{Rh}(100)$. $P(\text{CO}) = P(\text{NO}) = 8$ Torr.

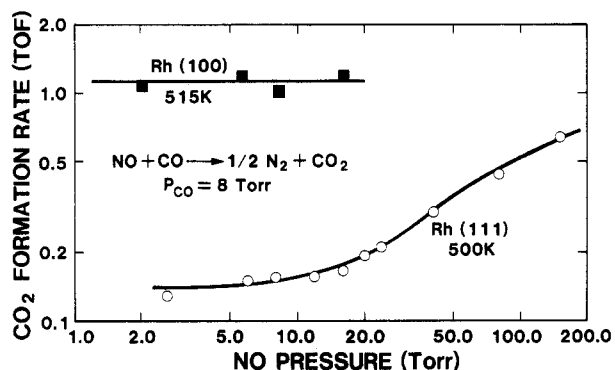


Figure 6. NO partial pressure dependence of the CO-NO reaction on $\text{Rh}(111)$ and $\text{Rh}(100)$. $P(\text{CO}) = 8$ Torr; $T[\text{Rh}(111)] = 500$ K; $T[\text{Rh}(100)] = 515$ K.

3.2. CO-NO Reaction. The Arrhenius plots for CO oxidation by NO on $\text{Rh}(100)$ and $\text{Rh}(111)$ are shown in Figure 5 for equal partial pressures of CO and NO (8.0 Torr). Significantly different activation energies ($\text{Rh}(111)$, 29 kcal/mol; $\text{Rh}(100)$, 24 kcal/mol) and specific activities were observed on the two surfaces, indicating that this reaction is sensitive to the geometric structure of the catalyst surface as previously proposed.⁹

The dependence of the reaction rate on the partial pressure of NO at ≈ 500 K and CO partial pressures of 8.0 Torr for the two single-crystal surfaces is shown in Figure 6. Similar NO pressure independence is observed on the two surfaces for NO pressures below 20 Torr. On $\text{Rh}(111)$, the reaction rate becomes positive order at higher NO partial pressures; the same behavior has been modelled quantitatively by Oh et al.⁹

The reaction orders with respect to CO partial pressure on $\text{Rh}(111)$ and $\text{Rh}(100)$ at ≈ 500 K and NO pressures of 8.0 Torr are illustrated in Figure 7. The data indicate little if any variation of the rate with changing CO pressures on either surface. Again, the lack of CO pressure dependence on $\text{Rh}(111)$ is consistent with the predictions of Oh et al.⁹

4. Discussion

4.1. CO-O_2 Reaction. The Arrhenius data shown in Figure 1 confirm that the CO-O_2 reaction is structure insensitive as has been previously suggested in studies on Rh ⁹ and other metals.^{10,11,17,18} The excellent agreement between the results obtained

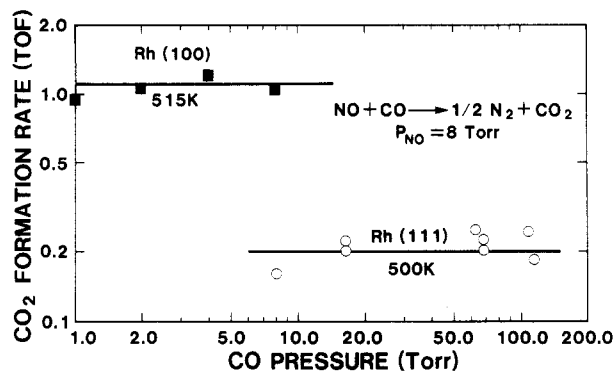


Figure 7. CO_2 formation rate from the CO-NO reaction on $\text{Rh}(111)$ and $\text{Rh}(100)$ as a function of CO partial pressure. $P(\text{NO}) = 8$ Torr; $T[\text{Rh}(111)] = 500$ K; $T[\text{Rh}(100)] = 515$ K.

on the single crystals and those rates measured on supported $\text{Rh}/\text{Al}_2\text{O}_3$ catalysts⁹ attests to the relevance of the model systems. In ref 9 it is shown that the quantitative agreement between the model single-crystal and supported catalysts extends not only to the Arrhenius rate data but to the kinetic order in CO and O_2 measured on both systems as well. As shown in Figures 2 and 4, the CO-O_2 reaction is approximately first order in O_2 and negative first order in CO pressures. Oh et al. have analyzed the kinetic data obtained on $\text{Rh}(111)$ and supported $\text{Rh}/\text{Al}_2\text{O}_3$ using a mathematical model which utilizes all of the elementary chemical processes (molecular and dissociative atomic adsorption, surface reaction, and desorption) occurring in the CO oxidation reaction, and their respective rates. The model predicts that, in the temperature and pressure range shown in Figures 2 and 4, the surface is predominantly covered by adsorbed CO and that the rate-controlling process is the dissociative chemisorption of O_2 . The order of the reaction with respect to the two reactants then reflects the ability of CO to compete more effectively for adsorption sites on the catalysts. This competitive adsorption may be responsible for recent observations by Cant and Angove¹⁹ that initially high reaction rates on supported Pt/SiO_2 catalysts can be correlated with a lower, non-steady-state coverage of CO obtained when the catalyst is first exposed to the reactants. The rate subsequently declines as the CO coverages increase to "equilibrium" values and steady-state reaction rates are observed.

Interesting changes in the reaction order are observed at high O_2/CO ratios as illustrated in Figure 2. The reaction is seen to deactivate at O_2 partial pressures greater than 75 Torr ($\text{O}_2/\text{CO} = 10:1$) and 230 Torr ($\text{O}_2/\text{CO} = 30:1$) for the $\text{Rh}(100)$ and $\text{Rh}(111)$ surfaces, respectively. Coincident with the change to negative-order O_2 pressure dependence, a sudden increase in the level of surface oxygen is observed on both surfaces (Figure 3). In studies on polycrystalline rhodium,²⁰ an inactive form of oxygen and/or oxide was hypothesized as responsible for lower reaction rates under net oxidizing conditions at low pressures. Oh and Carpenter²¹ determined that Rh_2O_3 was formed under similar conditions at high pressures on supported $\text{Rh}/\text{Al}_2\text{O}_3$ catalysts, again resulting in lower activities. This behavior was confirmed in a field-ion microscope/imaging atom-probe mass spectroscopic study on a Rh field emitter tip.²² Stoichiometric Rh_2O_3 was observed to grow on the emitter tip at O_2/CO ratios of 40/1 or greater. Thus, it seems likely that such an oxide growth on $\text{Rh}(100)$ and $\text{Rh}(111)$ is responsible for the rollover from positive to negative O_2 pressure dependence and for the increase in surface oxygen observed in Auger spectra taken subsequent to reaction.

We would like to understand why the O_2/CO reactant pressure ratios at which the reaction rate at 500 K rolls over and the surface oxygen coverage increases are lower on the $\text{Rh}(100)$ surface than on $\text{Rh}(111)$. One possible explanation is that the close-packed

(17) Peden, C. H. F.; Goodman, D. W. *J. Phys. Chem.* **1986**, *90*, 1360.

(18) Cant, N. W. *J. Catal.* **1980**, *62*, 173.

(19) Cant, N. W.; Angove, D. E. *J. Catal.* **1986**, *97*, 36.

(20) Kim, Y.; Shi, S.-K.; White, J. M. *J. Catal.* **1980**, *61*, 374.

(21) Oh, S. H.; Carpenter, J. E. *J. Catal.* **1983**, *80*, 472.

(22) Kellogg, G. L. *J. Catal.* **1985**, *92*, 167.

structure of the Rh(111) surface is more resistant to oxidation than is Rh(100). For Rh(100), the more open structure of the surface may lead to substantial oxidation of the near-surface region at a lower O₂/CO ratio which is, in turn, less reactive to CO. In this regard, it may be significant that while Rh(111)-oriented field emitter tips exhibited some increase in the size of the (111) planes upon CO-O₂ reaction, similar reaction on tips with (100) orientation displayed profound morphological changes.²³

4.2. CO-NO Reaction. The considerably different reaction rates for the CO-NO reaction on Rh(100) and Rh(111) surfaces (Figure 5) indicate that the reaction is sensitive to surface morphology as claimed previously by Oh et al., who measured significantly lower reaction rates and a considerably higher activation energy on a supported Rh/Al₂O₃ catalyst than on Rh(111).⁹ A model, similar to the one described earlier for the CO-O₂ reaction, was developed to account for the observed kinetics on Rh(111) and supported Rh. Quantitative agreement was obtained with measured kinetics on Rh(111), with the prediction that the surface is populated by a high concentration of adsorbed nitrogen atoms (N_a), and that the rate is limited by the formation of N₂ by a surface reaction between two adsorbed N atoms (β -N₂). The similarity between the activation energy of this surface reaction (31 kcal/mol)²⁴ and the apparent activation energy for the overall reaction (29 kcal/mol as shown in Figure 5) supports this conclusion. The model also predicts virtually no dependence of the rate on the CO pressure and moderate positive-order dependence on NO partial pressures, again in quantitative agreement with the rate measurements on Rh(111).⁹

The apparent activation energy of the CO-NO reaction on Rh(100) (24 kcal/mol; Figure 5) more closely resembles the barrier of about 21 kcal/mol measured for the surface reaction between adsorbed NO and N atoms (δ -N₂ formation) on both (111)²⁴ and (100)²⁵ surfaces. In addition, the recombination of N_a (β -N₂ formation) on Rh(100) occurs at a much higher temperature (\approx 770 K)²⁵ during TPD compared to Rh(111) (\approx 580 K)²⁴ and Rh(110) (\approx 660 K),²⁶ suggesting that this process is more highly activated and might be much less favorable during reaction on Rh(100). Were δ -N₂ formation determining the rate of the CO-NO reaction on Rh(100), the higher activity for the overall reaction on this surface would then imply that the prefactor for δ -N₂ formation on Rh(100) is considerably greater than on Rh(111) since the activation energy for this reaction is similar on both surfaces.^{24,25} If indeed δ -N₂ formation is rate-limiting on the (100) surface, the lack of dependence of the rate on NO pressure must then mean that the steady-state coverage of NO

on the surface during high-pressure reaction is approximately constant and does not depend on the partial pressure of NO in the pressure regime shown in Figure 6. Within this model, at much lower NO pressures, the reaction should become positive order in NO, although we do not have data to verify this.

A recent study of this reaction on Rh(100) has been reported²⁷ in which the kinetic data was adequately described by a model which only considered the β -N₂ pathway. While it is difficult to make a direct comparison between their data and our results due to differences in the partial and total pressures used in the two studies, it should be noted that the procedure to fit the model to the data in ref 27 treated the various rate constants as adjustable parameters. This method can be contrasted with the procedure used by Oh et al.⁹ which utilized values for the elementary steps of the reaction sequence determined separately in UHV surface science experiments to obtain fits with the overall kinetics.

5. Summary of Results

1. The CO-O₂ reaction is structure insensitive as demonstrated by the identical kinetics measured on Rh(111) and Rh(100) surfaces. Both surfaces deactivate at high O₂ partial pressures due to the formation of an inactive surface or bulk Rh oxide (probably Rh₂O₃).²² The deactivation occurs at a slightly lower O₂ partial pressure on Rh(100) possibly due to the relative ease of formation of the bulk oxide via diffusion of oxygen through this surface.²³

2. In contrast to the CO-O₂ reaction, the rate of CO oxidation by NO is dramatically different on the two single-crystal surfaces studied. This structure sensitivity was evident in the absolute rates and activation energies measured on Rh(111) and Rh(100). The kinetics on Rh(111) are well described by a kinetic model⁹ which predicts that the surface is predominantly covered by adsorbed N atoms and NO, and that the rate is limited by the surface reaction of N_a (β -N₂ formation) which frees up adsorption sites on the surface for the other reactants (notably CO). The reaction on Rh(100) may be rate-limited by δ -N₂ formation (NO_a + N_a → N₂ + O_a) due to the greater activation energy for β -N₂ formation on this surface.

Acknowledgment. The experimental work reported here was performed at Sandia National Laboratories and was supported by the U.S. Department of Energy, Office of Basic Energy Sciences, Division of Chemical Sciences (contract no. DE-AC04-76DP00789). We also acknowledge the contribution to this work of the late Kent Hoffman who performed some of the initial experiments.

Registry No. Rh, 7440-16-6; NO, 10102-43-9; O₂, 7782-44-7; CO, 630-08-0.

(23) Kellogg, G. L. *J. Vac. Sci. Technol. A* **1986**, *4*, 1419.

(24) Root, T. W.; Schmidt, L. D.; Fisher, G. B. *Surf. Sci.* **1983**, *134*, 30.

(25) Fisher, G. B.; DiMaggio, C. L.; Schmieg, S. J., to be submitted for publication.

(26) Baird, R. J.; Ku, R. C.; Wynblatt, P. *Surf. Sci.* **1980**, *97*, 346.

(27) Hendershot, R. E.; Hansen, R. S. *J. Catal.* **1986**, *98*, 150.